

Multiple nearest-neighbor exchange model for the frustrated magnetic molecules $\{\text{Mo}_{72}\text{Fe}_{30}\}$ and $\{\text{Mo}_{72}\text{Cr}_{30}\}$

Christian Schröder*

*Department of Electrical Engineering and Computer Science,
University of Applied Sciences Bielefeld, D-33602 Bielefeld,
Germany & Ames Laboratory, Ames, Iowa 50011, USA*

Ruslan Prozorov, Paul Kögerler, Matthew D. Vannette, Xikui Fang, and Marshall Luban
Ames Laboratory & Department of Physics and Astronomy, Iowa State University, Ames, Iowa 50011, USA

Akira Matsuo and Koichi Kindo

*Institute for Solid State Physics, University of Tokyo,
Kashiwanoha 5-1-5, Kashiwa, Chiba 277-8581, Japan*

Achim Müller and Ana Maria Todea

Fakultät für Chemie, Universität Bielefeld, D-33501 Bielefeld, Germany

(Dated: October 22, 2018)

Our measurements of the differential susceptibility $\partial M/\partial H$ of the frustrated magnetic molecules $\{\text{Mo}_{72}\text{Fe}_{30}\}$ and $\{\text{Mo}_{72}\text{Cr}_{30}\}$ reveal a pronounced dependence on magnetic field (H) and temperature (T) in the low H - low T regime, contrary to the predictions of existing models. Excellent agreement with experiment is achieved upon formulating a nearest-neighbor classical Heisenberg model where the 60 nearest-neighbor exchange interactions in each molecule, rather than being identical as has been assumed heretofore, are described by a two-parameter rectangular probability distribution of values of the exchange constant. We suggest that the probability distribution provides a convenient phenomenological platform for summarizing the combined effects of multiple microscopic mechanisms that disrupt the idealized picture of a Heisenberg model based on a single value of the nearest-neighbor exchange constant.

PACS numbers: 75.10.Jm, 75.10.Hk, 75.40.Cx, 75.50.Xx, 75.50.Ee

Keywords: Quantum Spin Systems, Classical Spin Models, Magnetic Molecules, Heisenberg model, Frustration

I. INTRODUCTION

In recent years there has been extensive research on magnetic molecules as these are novel, realizable systems for exploring magnetic phenomena in low-dimensional magnetic materials.^{1,2,3,4,5} Among these diverse systems the pair of Keplerate structural type magnetic molecules abbreviated as $\{\text{Mo}_{72}\text{Fe}_{30}\}$ and $\{\text{Mo}_{72}\text{Cr}_{30}\}$, each hosting a highly symmetric array of 30 exchange-coupled magnetic ions (“spin centers”), serve as highly attractive targets for the investigation of frustrated magnetic systems. In these molecules^{6,7} the magnetic ions Fe^{III} (spin $s = 5/2$) and Cr^{III} (spin $s = 3/2$) occupy the 30 symmetric sites of an icosidodecahedron, a closed spherical structure consisting of 20 corner-sharing triangles arranged around 12 pentagons (diamagnetic polyoxomolybdate fragments). This is a zero-dimensional analogue of the planar kagome lattice that is composed of corner-sharing triangles arranged around hexagons. A useful theoretical framework that has been employed^{8,9,10} in studying these magnetic molecules is based on an isotropic Heisenberg model, where each magnetic ion is coupled via intra-molecular isotropic antiferromagnetic exchange to its four nearest neighbor magnetic ions, and all of the 60 intra-molecular exchange interactions are

of equal strength (henceforth, “single- J model”).¹¹ Unfortunately the quantum Heisenberg model of the two magnetic molecules is intractable using either analytical or matrix diagonalization methods. Nevertheless, the nearest-neighbor exchange constant for each molecule has been established by comparing experimental data above 30 K for the temperature-dependent zero-field susceptibility with data obtained by simulational methods using the quantum⁷ and classical⁹ Monte Carlo methods. For temperatures below about 30 K, where the quantum Monte Carlo method proves to be ineffective for the two magnetic molecules due to frustration effects,¹² the classical Heisenberg model is at present the only practical platform for establishing the dependence of the magnetization $M(H, T)$ on external magnetic field H and temperature T . A rigorous analytical result⁸ for the classical, nearest-neighbor, single- J Heisenberg model states that, in the zero temperature limit, M is linear in H until M saturates (saturation fields $H_s = 17.7$ T and 60.0 T for $\{\text{Mo}_{72}\text{Fe}_{30}\}$ and $\{\text{Mo}_{72}\text{Cr}_{30}\}$, respectively). The practical relevance of the classical Heisenberg model in describing these magnetic molecules even at low temperatures was strikingly demonstrated in an earlier experiment⁹ on $\{\text{Mo}_{72}\text{Fe}_{30}\}$ at 0.4 K, showing an overall linear dependence of M on H and its saturation at approximately 17.7 T. The ground state envisaged by the classical single-

J model is characterized by high-symmetry spin frustration. In particular, for $H = 0$, in the ground state the spins are coplanar with an angular separation of 120° between the orientations of nearest-neighbor spins. On increasing the external field H the spin vectors gradually tilt towards the field vector, until full alignment is achieved when $H = H_s$, while their projections in the plane perpendicular to the field vector retain the 120° pattern for nearest-neighbor spins.⁸ It would be reasonable to expect that $M(H, T)$ is an analytic function of its variables and thus $\partial M/\partial H \approx M_s/H_s$ for $H < H_s$ and $k_B T \ll J_0$, essentially independent of *both* H and T in these intervals, where J_0 is the exchange constant of the single- J classical Heisenberg model.¹¹ Indeed our classical Monte Carlo calculations confirm this behavior.

As shown here, new and crucial features of $M(H, T)$ become accessible upon examining the differential susceptibility, $\partial M/\partial H$, as a function of H and T . What emerge are significant conflicts, spelled out in Secs. II A and II B between the results of our measurements and a theory based on the classical single- J model as concerns both the T and H dependence of $\partial M/\partial H$ below 5 K. However, and this is the central idea of this paper, agreement with experiment is achieved upon adopting a refined classical Heisenberg model of $\{\text{Mo}_{72}\text{Fe}_{30}\}$ and $\{\text{Mo}_{72}\text{Cr}_{30}\}$, where we drop the assumption of a single, common value for the nearest-neighbor exchange constant, using instead a rectangular probability distribution¹⁵ for the 60 nearest-neighbor intra-molecular interactions.

The layout of this paper is as follows. In Sec. II A we present our experimental results for $\partial M/\partial H$ as a function of T in the low-temperature range for $\{\text{Mo}_{72}\text{Fe}_{30}\}$ and $\{\text{Mo}_{72}\text{Cr}_{30}\}$ for several low field values. In Sec. II B we present our experimental results for $\partial M/\partial H$ as a function of H . In Sec. III we show that the model system of a classical isosceles spin triangle exhibits the same qualitative features as the results of our experiments summarized in Sec. II A. In Sec. IV, using the classical Heisenberg model of the icosidodecahedron and Monte Carlo simulational methods, we show that excellent agreement between a model calculation based on a two-parameter distribution of exchange constants and our experimental data of Sec. II can be achieved. Finally, in Sec. V we summarize our findings, discuss the broader implications of our results, and identify several open questions.

II. EXPERIMENT

A. $\partial M/\partial H$ versus T

Measurements of $\partial M/\partial H$ versus T were performed at Ames Laboratory on polycrystalline samples of $\{\text{Mo}_{72}\text{Fe}_{30}\}$ and $\{\text{Mo}_{72}\text{Cr}_{30}\}$ (see experimental sections of Refs. 6 and 7) prepared by employing optimized synthesis methods and re-crystallization steps to minimize

paramagnetic impurities. Our data was obtained by using a self-resonating LC circuit driven by a tunnel diode.^{18,19} Briefly, a tank circuit consisting of a small coil of inductance L_0 and a capacitor, C , is kept at constant temperature of 5 ± 0.005 K. The sample is mounted on a sapphire holder, which is inserted into the coil without making contact. In the absence of the sample, the circuit resonates at the resonant frequency $2\pi f_0 = 1/\sqrt{LC}$. When a sample with susceptibility χ is inserted into the coil, the resonant frequency changes from f_0 to $f(\chi)$ due to the change of the coil inductance, $L = d\Phi/dI$, where Φ is the total magnetic flux through the coil and I is the current in the coil. This current generates a magnetic field of about 20 mOe. If the magnetic perturbation due to the sample is small, the shift of the resonant frequency

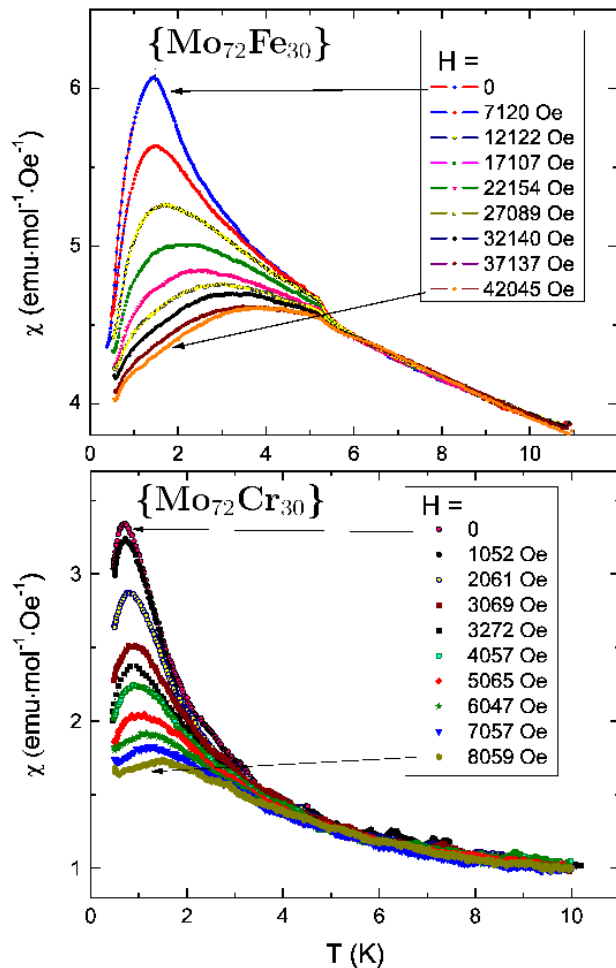


FIG. 1: Temperature dependence of the measured differential susceptibility $\partial M/\partial H$ for $\{\text{Mo}_{72}\text{Fe}_{30}\}$ (upper panel) and for $\{\text{Mo}_{72}\text{Cr}_{30}\}$ (lower panel). Values of H are listed in the legends.

is given by

$$\frac{\Delta f}{f_0} \approx \frac{\Delta L(\chi)}{2L_0} = \frac{4\pi\chi}{(1-N)} \frac{V}{2V_0}.$$

Here N is the demagnetization factor, $\Delta L(\chi) = |L(\chi) - L_0| \ll L_0$ is the change of the coil inductance, V is the sample volume and V_0 is volume of the coil, and χ is the dynamic magnetic susceptibility at our typical resonant frequency of 10 MHz. This frequency is still much lower than characteristic frequencies and the response can be considered as static, i.e., χ can be identified with $\partial M/\partial H$. Measured frequency shifts for the samples described in this work are of the order of 1 to 10 Hz, whereas the experimental resolution of the setup is about 0.01 Hz which corresponds to a smallest detectable magnetic moment of about 5 picoemu. For easy comparison with other experiments, the measured frequency shift is proportional to the change in the total magnetic moment of the sample at a given frequency, $\Delta M = C\Delta f$, where C is a calibration constant.

In Fig. 1 we show our experimental data for $\partial M/\partial H$ versus T for $\{\text{Mo}_{72}\text{Fe}_{30}\}$ and $\{\text{Mo}_{72}\text{Cr}_{30}\}$, respectively. The calibration of the experimental data was achieved by matching the effective magnetic moment inferred from the measured frequency shift to low-field (3 - 50000 Gs) ac (10 to 1000 Hz) and dc susceptibility measurements performed on a Quantum Design MPMS, which show that at high temperatures dynamic effects can be neglected. The assumption of static behavior is supported by the fact that all curves collapse onto each other for $T > 5$ K. The most striking feature of these data is the very strong dependence of $\partial M/\partial H$ on H and T . As remarked in Sec. I, this behavior is contrary to that predicted by the single- J model, specifically $M \approx H\chi_0(k_B T/J_0) \approx H\chi_0(0)$, that is, $\partial M/\partial H$ is independent of H and T in the regime $H \ll H_s$, $k_B T \ll J_0$.

B. $\partial M/\partial H$ versus H

In Fig. 3 we show our experimental data for $\partial M/\partial H$ versus H for both $\{\text{Mo}_{72}\text{Fe}_{30}\}$ (upper panel) and $\{\text{Mo}_{72}\text{Cr}_{30}\}$ (lower panel). These data sets were obtained by measuring the magnetization using pulsed magnetic fields (typical sweep rate 15000 T/s) with a standard inductive method at facilities of Okayama University, Tohoku University, and University of Tokyo. Also shown are the corresponding classical Monte Carlo simulational results for the single- J model (dashed curve) for the indicated temperatures.

The inadequacy of the single- J model is striking in that the simulational data differ from the experimental data in four important ways. *First*, the experimental data exhibit a steep rise for decreasing low fields, and the lower the temperature the steeper the rise. This is consistent with our experimental findings in Sec. II A for the T -dependence of $\partial M/\partial H$. These features are entirely absent for the single- J model; in particular, $\partial M/\partial H$ is

essentially independent of field in the low-field regime. *Second*, the local minimum in the experimental data is significantly broader than that predicted by the single- J model. *Third*, according to the single- J model a local minimum in $\partial M/\partial H$ versus H emerges at $T = 0$ K at a field $H = H_s/3$ (approx. 6 T and 20 T for $\{\text{Mo}_{72}\text{Fe}_{30}\}$ and $\{\text{Cr}_{72}\text{Fe}_{30}\}$, respectively) and it is enhanced with increasing T .¹⁷ By contrast, our experimental data for fields in the vicinity of $H_s/3$ differ insignificantly with temperature. *Fourth*, for $\{\text{Mo}_{72}\text{Fe}_{30}\}$ the experimental data for 0.42 K shows a decrease with increasing field above 10 T, quite distinct from the pattern of the single- J model.

III. CLASSICAL ISOSCELES SPIN TRIANGLES

In this Section we give a qualitative explanation for our experimental findings in Sec. II A. We suggest that

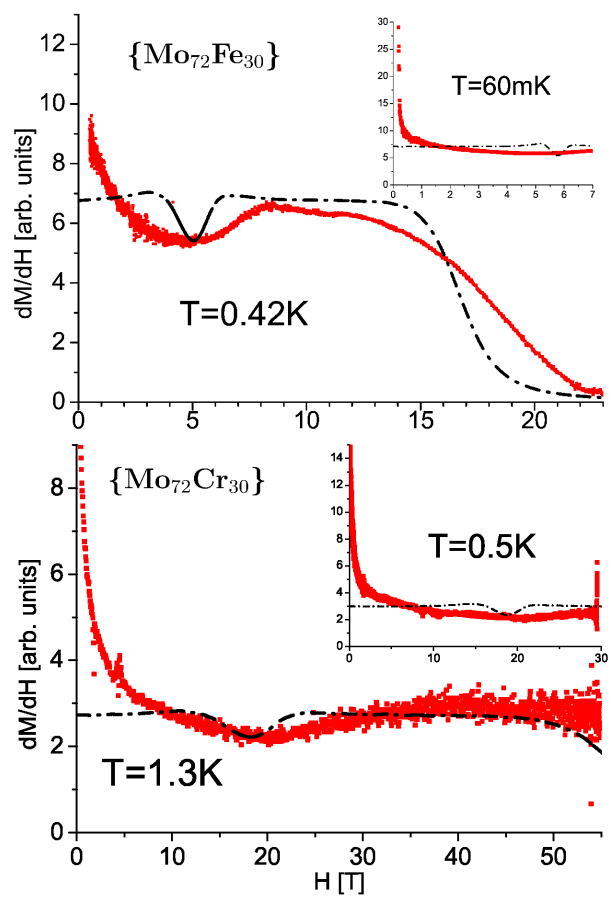


FIG. 2: Magnetic field dependence of the measured differential susceptibility $\partial M/\partial H$, shown in red, for $\{\text{Mo}_{72}\text{Fe}_{30}\}$ for $T = 0.42$ K and 60 mK (upper panel, inset) and for $\{\text{Mo}_{72}\text{Cr}_{30}\}$ for $T = 1.3$ K and 0.5 K (lower panel, inset). The dashed curves are the results of the single- J model for these temperatures.

the strong sensitivity of the differential susceptibility on H and T reflects a non-analytic dependence of the magnetization on these variables, a characteristic already exhibited by independent classical isosceles spin triangles. The Hamiltonian of a spin triangle is given in footnote 16 in terms of dimensionless quantities. In particular, the three pair-wise interactions are described by two different antiferromagnetic exchange constants (positive values of J and J') and we consider both cases, $J' < J$ and $J' > J$.

For the equilateral spin triangle ($J' = J = J_0$) at $T = 0$ K the magnetic moment per triangle, $M(H, 0)$, is a continuous, linear function of H and, in particular, it vanishes for $H \rightarrow 0$. Specifically, $M(H, 0) = 3H/H_s$ for $-H_s < H < H_s$, where $H_s = 3J_0$ is the saturation field.

Analytical calculation of $M(H, 0)$ for the corresponding isosceles spin triangle is a non-trivial task for general values of J/J' as it is necessary to carefully identify the configuration of least energy for arbitrary values of H . The final results are as follows: For the case $J' > J$: $M(H > 0, 0) = 1 - J/J' + (2 + J/J')H/H_s$ for $0 < H < H_s$, where $H_s = 2J' + J$ is the saturation field. For the case $J' < J < 2J'$: $M(H > 0, 0) = J/J' - 1 + H/J'$ for $0 < H < 2J' - J$; $M(H, 0) = 1$ for $2J' - J < H < J$; and $M(H, 0) = H/J$ for $J < H < 3J = H_s$. $M(H, 0)$ is subject to the antisymmetry property $M(-H, 0) = -M(H, 0)$. The discontinuous behavior for $H \rightarrow 0$ is of particular importance in both cases. Although this discontinuity occurs only at 0 K, it is the crucial mechanism responsible for the great sensitivity of $M(H, T)$ in the low H - low T regime.

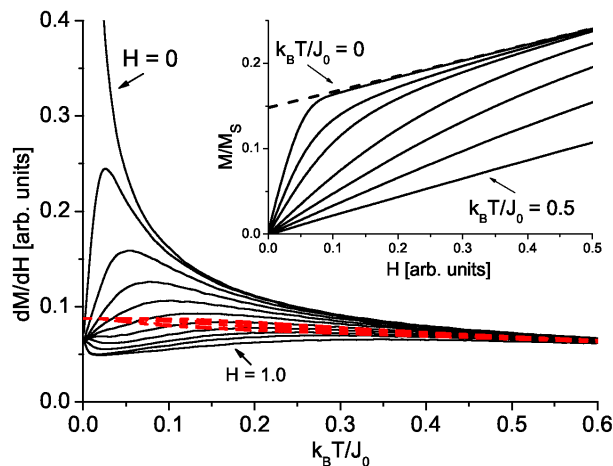


FIG. 3: Temperature dependence of the differential susceptibility $\partial M/\partial H$ for a classical isosceles spin triangle (black curves) with $J/k_B = 1$ K and $J'/k_B = 1.8$ K for field values $H = 0, 0.1, \dots, 1$. Inset: M/M_s versus H for the values $k_B T/J_0 = 0, 0.001, 0.01, 0.02, 0.05, 0.1, 0.2, 0.5$. Results for the corresponding classical equilateral spin triangle ($J_0/k_B = 1.267$) K are given by the red dashed curves.

The form of $M(T, H)$ for finite T can, in principle,

be derived for this model system by analytical methods, however these calculations are substantially more intricate than for the classical equilateral spin triangle (see Sec. II B of O. Ciftja *et al.* listed in Ref. 11). For practical purposes, the simplest procedure is to use the classical Monte Carlo method for convenient numerical choices of J'/J . In Fig. 3 we display our results for the choices $J/k_B = 1$ K, $J'/k_B = 1.8$ K. The most important feature to note is that while M is indeed a continuous function of H for any nonzero T , the quantity $\partial M/\partial H$, provided in the main portion of Fig. 3, exhibits strong temperature dependence for weak magnetic fields. Indeed, the curves fan with increasing H in a manner that is strikingly similar to that shown in Fig. 1. Similar behavior occurs for cases where $J' < J$. By contrast, for the corresponding classical equilateral spin triangle $\partial M/\partial H$ is virtually independent of T , as is seen in Fig. 3.

IV. MULTIPLE NEAREST-NEIGHBOR COUPLINGS

The T and H dependence of $\partial M/\partial H$ for the classical isosceles spin triangle considered in the previous section is remarkably similar to that of our experimental data in Sec. II. However, to achieve a more realistic model, in the following we assume that the 60 nearest-neighbor exchange interactions between magnetic ions in a given molecule are characterized by a probability distribution with two adjustable width parameters. In the following Section we rationalize the use of a probability distribution as a convenient way for summarizing the combined effects of multiple microscopic mechanisms that disrupt the use of an idealized, single- J model.

We simulate each of $\{\text{Mo}_{72}\text{Fe}_{30}\}$ and $\{\text{Mo}_{72}\text{Cr}_{30}\}$ by considering an ensemble of up to 100 independent systems, for a total of 60 couplings per system. We assign values of the 6000 exchange constants using a random number generator according to the following rules: 1) The average value, J_{0n} , of the classical exchange constant (in units of Boltzmann's constant) for the n th system is allowed to assume any value in the interval $((1 - \tau)J_0, (1 + \tau)J_0)$ with equal probability, where J_0 is chosen as 13.74 K for $\{\text{Mo}_{72}\text{Fe}_{30}\}$ and 32.63 K for $\{\text{Mo}_{72}\text{Cr}_{30}\}$ as determined by high-temperature susceptibility measurements¹¹; 2) For the n th system, the individual values of the classical exchange constant are allowed to assume any value in the interval $((1 - \rho)J_{0n}, (1 + \rho)J_{0n})$ with equal probability. For each molecule the two parameters τ, ρ characterizing these rectangular probability distributions were determined so as to provide an optimal fit with our experimental data for $\partial M/\partial H$ versus H .

In Fig. 4 we present our results for $\partial M/\partial H$ versus H for $\{\text{Mo}_{72}\text{Fe}_{30}\}$ and $\{\text{Mo}_{72}\text{Cr}_{30}\}$. Note the excellent agreement between the experimental data and the simulation results obtained using our multiple- J model (solid curve). In the case of $\{\text{Mo}_{72}\text{Fe}_{30}\}$, the opti-

mal choices of the parameters τ , ρ were $\tau = 0.15$ and $\rho = 0.40$, whereas for $\{\text{Mo}_{72}\text{Cr}_{30}\}$ these were $\tau = 0$ and $\rho = 0.5$.

The motivation for using two distributions as described above is the following. One can attribute the influence of the two distributions, characterized by τ and ρ , respectively, to complementary effects which only *in combination* lead to the observed properties of both molecules. The value of τ controls the variation in the values of the mean exchange constant *per molecule*, which leads to variations in the value of the saturation field H_s and hence in the value of the minimum in $\partial M/\partial H$ versus H at $H_s/3$. By averaging over those variations one finds that $\partial M/\partial H$ versus H starts to decrease at a much lower value of H than predicted by the single- J model and *simultaneously* finds that the minimum at $H_s/3$ is broadened as observed. However, using this distribution alone one cannot explain the observed strong H dependence of $\partial M/\partial H$ in the low T - low H regime, because each

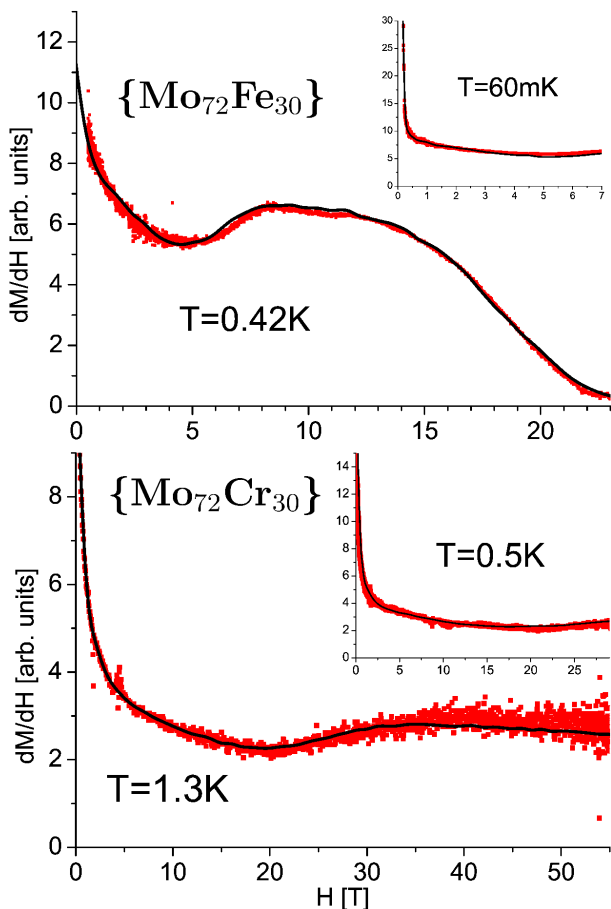


FIG. 4: Measured differential susceptibility $\partial M/\partial H$ versus H , shown in red, for $\{\text{Mo}_{72}\text{Fe}_{30}\}$ for $T = 0.42$ K and 60 mK (inset) and for $\{\text{Mo}_{72}\text{Cr}_{30}\}$ for $T = 1.3$ K (inset: 0.5 K) and simulational results (solid black curve) using a multiple- J model for the optimal choice of the probability distribution parameters as given in the text.

molecule is still characterized by a single exchange constant. Introducing a second distribution, characterized by the parameter ρ , leads to a variation in the values of the exchange constant *within a molecule* with the effect that the corner-sharing spin triangles are of the scalene-type rather than equilateral-type. This gives rise to the non-analytic behavior of the magnetization at $H = 0$ for 0 K and hence to the characteristic effects we have found in the low H - low T regime. In our simulations we have studied a very large range of choices of parameter pairs. The optimal choice for $\{\text{Mo}_{72}\text{Fe}_{30}\}$ can be narrowed to $\tau = 0.15 \pm 0.02$ and $\rho = 0.40 \pm 0.02$. For $\{\text{Mo}_{72}\text{Cr}_{30}\}$ we find $\rho = 0.50 \pm 0.02$, however τ can be chosen in the range 0 to 0.2 without any observable effect. This is due to the fact that for $\{\text{Mo}_{72}\text{Cr}_{30}\}$ magnetization measurements above the saturation field ($H_s = 60$ T) are not achievable at the present time. In the case of $\{\text{Mo}_{72}\text{Fe}_{30}\}$, for which $H_s = 17.7$ T, the availability of magnetization data above the saturation field allows for a greatly reduced uncertainty in the value of τ .

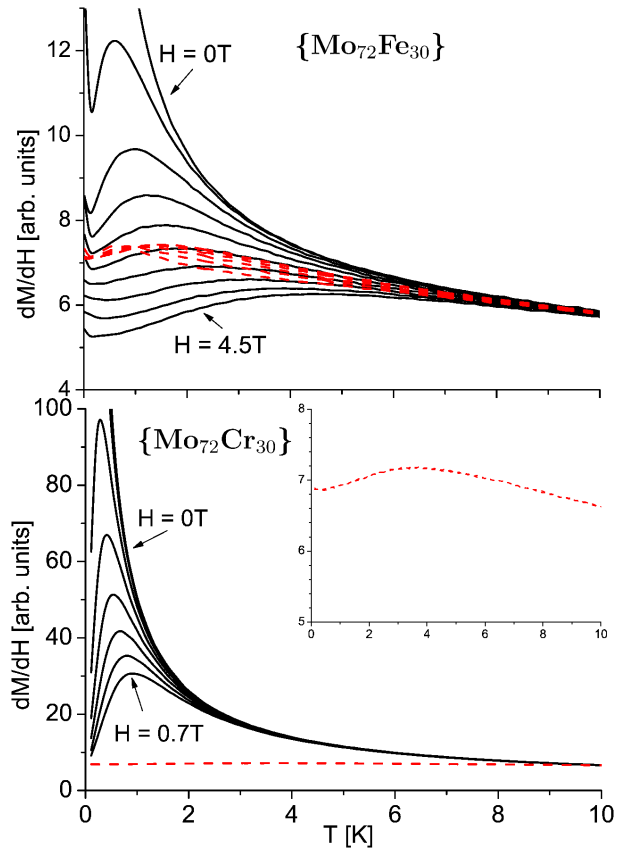


FIG. 5: Simulational results for $\partial M/\partial H$ versus T based on the multiple- J model using the optimal distribution parameters for $\{\text{Mo}_{72}\text{Fe}_{30}\}$ and for $\{\text{Mo}_{72}\text{Cr}_{30}\}$ as given in the text. Results for the corresponding single- J model calculations are shown as red dashed curves.

Shown in Fig. 5 are our simulational results for $\partial M/\partial H$ versus T for several different values of H using

the probability distribution with optimal parameters appropriate for $\{\text{Mo}_{72}\text{Fe}_{30}\}$ and $\{\text{Mo}_{72}\text{Cr}_{30}\}$. These results (black curves) are strikingly similar to the experimental curves seen in Fig. 1; the corresponding curves (shown in red) for the single- J model, for the same choice of the mean value J_0 , are essentially indistinguishable from one another. This again strongly supports the existence of the multiple- J scenario. Note that, in the experiment as well as in the simulations, with increasing temperature the curves for different field values rapidly converge and become indistinguishable from one another. Also, for increasing temperature, the results for the multiple- J model merge with those of the single- J model, as expected, since the average exchange constant across the ensemble, J_0 , is chosen to equal to the exchange constant of the single- J model. Finally, it remains to be seen whether the sharp rise in the curves of the upper panel of Fig. 5 below 200 mK is an experimental feature in $\{\text{Mo}_{72}\text{Fe}_{30}\}$ or merely an artifact of the multiple- J model based on a rectangular probability distribution.

V. SUMMARY AND DISCUSSION

In this article, we have presented our experimental data for the differential susceptibility of the pair of magnetic molecules $\{\text{Mo}_{72}\text{Fe}_{30}\}$ and $\{\text{Mo}_{72}\text{Cr}_{30}\}$ as a function of magnetic field and temperature. Below 5 K these data are strikingly different from what can be provided using a classical Heisenberg model with a single value of the nearest-neighbor exchange constant (single- J model). We have achieved excellent agreement with our experimental data upon adopting a classical Heisenberg model where the 60 nearest-neighbor interactions are not identical; instead, the values of the exchange constants are described by a two-parameter probability distribution with a mean value as determined from experimental $\partial M/\partial H$ data above 30 K using the single- J model. Above 5 K the single- J model provides a satisfactory description of each molecule.

Since the icosidodecahedron structure consists of corner-sharing triangles, it is not surprising that the Heisenberg model of *independent* classical isosceles spin triangles provides a simple yet instructive model in that it exhibits the main qualitative features of our experimental data. We note here that a similar approach has been employed successfully for various two-dimensional spin systems on triangular lattices²⁰. For example, in the case of manganese tricyanomethanide the so-called ‘row model’ based on *connected* isosceles triangles provides the explanation for an unusual magnetic-field dependence of the spin ordering²⁴. In the context of independent classical isosceles spin triangles one can figuratively describe the effect of multiple exchange constants as modifying the spin frustration from the standard 120° angular separation between spin vectors of the equilateral spin triangle. The operational consequence is that the magnetization, for $T = 0$, of an isosceles spin triangle is a non-analytic

function of magnetic field for $H = 0$, and this is manifested in $\partial M/\partial H$ being a highly sensitive function of its arguments for small H and T .

The existence of a distribution of nearest-neighbor exchange constants can be expected to be responsible for a significant lifting of degeneracies of magnetic energy levels. To be specific, the quantum rotational band model¹⁰, which is a solvable alternative to the nearest-neighbor single- J quantum Heisenberg model, predicts a discrete spectrum of energy levels, many of which have a very high degeneracy due to large multiplicity factors. Perturbing this model Hamiltonian by using a distribution of J -values would remove a major fraction of these degeneracies. The lifting of level degeneracies could provide a reasonable explanation for three long-standing puzzling issues concerning these magnetic molecules: The first issue is the very broad peak (maximum at 0.6 meV) that has been observed by inelastic neutron scattering on $\{\text{Mo}_{72}\text{Fe}_{30}\}$ at 65 mK. In order to qualitatively reproduce the observed peak using the rotational band model, it was necessary in Ref. 21 to perform the calculations upon assigning a large energy width (0.3 meV) for the individual energy levels. We suggest that the source of this large energy width might be the lifting of the majority of degeneracies associated with a single- J model.

A second important consequence of the splitting of highly degenerate levels would be that the molecules could exhibit classical characteristics down to very low temperatures. This would provide a very reasonable explanation for the surprising fact that our simulational results based on the *classical* Heisenberg Hamiltonian are so successful in describing $\{\text{Mo}_{72}\text{Cr}_{30}\}$, despite the fact that the Cr^{III} ions have a small spin ($3/2$). Stated differently, with the lifting of degeneracies and the fanning out of energy levels the effective temperature for the crossover from classical to quantum behavior can be anticipated to be considerably lower than that expected *a priori* for the single- J model.

Third, the failure of efforts to observe magnetization steps, in measurements of magnetization versus H , in the mK temperature range in both $\{\text{Mo}_{72}\text{Fe}_{30}\}$ and $\{\text{Mo}_{72}\text{Cr}_{30}\}$ could also be attributed to the removal of degeneracies of the magnetic energy levels. The occurrence of magnetization steps at low temperatures is associated with the field-induced crossing of successive energy levels of the lowest rotational band. However, a discrete level associated with total spin quantum number S has multiplicity $2S+1$ [total degeneracy $(2S+1)^2$]. If this degeneracy is lifted there will be a multitude of level crossings at slightly different field values and thus give rise to blurred effects down to lower temperatures than would otherwise be expected.

Given the finite-spin values of the Fe^{III} and Cr^{III} ions, is it possible to explain the present experimental findings based on a *quantum* Heisenberg model that adopts a common, *single* value of the exchange constant for all of the nearest-neighbor interactions? We strongly doubt that this is possible, for we have seen, albeit with a *clas-*

sical Heisenberg model, that it is the spread in values of the nearest-neighbor exchange constant that fuels the sensitive dependence of $\partial M/\partial H$ on T , or equivalently the non-analytic behavior of magnetization on H in the low H - low T regime.

Basing our simulations on a probability distribution for the nearest-neighbor exchange interaction has led to excellent agreement with the detailed features of our experimental data including the sensitive dependence of $\partial M/\partial H$ on T and H . One can attribute the failure of the single- J model to the combined effect of a large number of diverse perturbing mechanisms. The effects of impurities, variations in the exchange-coupling geometry, weak magnetic exchange interactions of more-distant neighbors, Dzyaloshinsky-Moriya and dipole-dipole interactions in these magnetic molecules are some of the many effects that are excluded when one uses an idealized single- J model. On the other hand, it is at this stage an extremely difficult, essentially impossible task to realistically quantify the effects of the diverse mechanisms. A theoretical description based on a Heisenberg model where the nearest-neighbor exchange constant is chosen using a probability distribution provides a relatively simple, phenomenological platform for compromising between the need for microscopic realism versus practical limitations. Ultimately it is significant that a two-parameter probability description can actually provide the level of agreement that we have found. Finally, we remark that other choices of probability distributions can be expected to perform equally well.

As one example of the complications in assessing the plethora of perturbing mechanisms, we consider the variation in the intramolecular distances between nearest-neighbor magnetic ions. A geometric analysis utilizing existing low-temperature single crystal X-ray structure data for $\{\text{Mo}_{72}\text{Fe}_{30}\}$ molecules shows that the substructure of the magnetic ions is close to an ideal I_h -symmetric geometry. There is a standard deviation of 0.04525 Å (0.70%) and a maximum deviation of 1.4% from the average Fe-Fe distance of 6.4493 Å for all 60 Fe-Fe nearest-neighbor distances. Besides the distances between the spin centers, geometric variations within the polyoxomolybdate exchange ligand are observed. In particular the O-Mo-O bond angle variations should affect the total orbital overlap and thus the exchange energy due to the spatially anisotropic character of the (unoccupied) Mo(4d) orbitals. For $\{\text{Mo}_{72}\text{Fe}_{30}\}$, an angular range 103.6° – 106.6° is observed, which in part is caused by crystallographic disorder of Mo positions. To assess the influence of various geometric parameters involved in the superexchange pathways between two nearest-neighbor spin centers, both binding to a pentagonal diamagnetic $[\text{Mo}_6^{\text{VI}}\text{O}_{21}(\text{H}_2\text{O})_6]^{6-} = \{\text{Mo}_6\}$ fragment, we performed systematic Density Functional Theory-Broken Symmetry calculations²² on a model system in which two $s = 1/2$ $[\text{V}^{\text{IV}}\text{O}(\text{H}_2\text{O})_2]^{2+}$ groups are coordinated to such a $\{\text{Mo}_6\}$ fragment in a nearest-neighbor (1,2) configuration. The fragment is augmented by an additional

$\text{Zn}^{\text{II}}(\text{H}_2\text{O})_4$ group binding in a (1,3,5) configuration for charge neutrality. The geometry of this model system was adjusted to match the actual configurations occurring in $\{\text{Mo}_{72}\text{Fe}_{30}\}$. We find that J in such a model system can deviate by up to $\pm 8\%$ from the average value J_0 . Given the similarity between VO^{2+} , Cr^{III} , and Fe^{III} in the Keplerate systems, namely that the magnetic orbitals cause a nearly isotropic spin density distribution, we expect that the variations in the relative values of J span a very similar interval for $\{\text{Mo}_{72}\text{Fe}_{30}\}$ and $\{\text{Mo}_{72}\text{Cr}_{30}\}$. As the intra-molecular variation in the values of the nearest-neighbor exchange constants implied by the optimal values (given in Sec. IV) of the parameter ρ are significantly larger, we suggest that this is due to numerous other perturbing mechanisms, some of which we listed above.

We also note that other attempts to explain limited features of $\partial M/\partial H$, specifically the broadening of the minimum versus H for $\{\text{Mo}_{72}\text{Fe}_{30}\}$, have been considered in the literature. One attempt assumed an elevated spin temperature during the pulsed field measurements, however this could be ruled out since a subsequent steady-field measurement reproduced the results obtained by the pulsed-field technique.¹⁷ Second, in a simulational study based on classical Monte Carlo calculations, effects of magnetic anisotropies, Dzyaloshinsky-Moriya, and dipole-dipole interactions have been considered.²³ However, our own comprehensive simulational studies of these same mechanisms have shown that they give rise to only very minor corrections on the width of the minimum in $\partial M/\partial H$ versus H for any reasonable choices of model parameters.

Finally, we suggest the additional possibility that in these molecules the variation of the exchange interaction is spontaneously generated so as to lower the system's magnetoelastic energy. Such behavior has been observed experimentally and described theoretically for a variety of antiferromagnetic oxide pyrochlore compounds^{25,26,27,28}. The pyrochlore lattice consists of corner-sharing tetrahedra and exhibits geometric frustration. In this regard one can understand this structure as the three-dimensional 'cousin' of the corner-sharing triangle type structures realized in $\{\text{Mo}_{72}\text{Fe}_{30}\}$ and $\{\text{Mo}_{72}\text{Cr}_{30}\}$.

In any event, it is highly satisfying that the frustrated magnetic molecules $\{\text{Mo}_{72}\text{Fe}_{30}\}$ and $\{\text{Mo}_{72}\text{Cr}_{30}\}$, ostensibly zero-dimensional systems, are a source of novel and intriguing magnetic behavior.

Acknowledgments

Research performed by C.S. at the Applied Sciences University Bielefeld was supported by an institutional grant. Work at the Ames Laboratory was supported by the Department of Energy-Basic Energy Sciences under Contract No. DE-AC02-07CH11358. R.P. acknowledges financial support from the Alfred P. Sloan Foundation. A.M. thanks the Deutsche Forschungsgemein-

schaft, the Fonds der Chemischen Industrie, and the European Union for financial support. We thank H. Nojiri for sharing experimental data with us and for helpful discussions. We also thank the thousands of volunteers participating in the public resource computing fac-

ility, Spinhenge@home [<http://spin.fh-bielefeld.de>]. The large-scale Monte Carlo simulations necessary for the present research were made possible due to the availability of their personal computers.

-
- * Electronic address: christian.schroeder@fh-bielefeld.de
- ¹ O. Kahn, *Molecular Magnetism* (VCH, Weinheim, 1993).
 - ² D. Gatteschi, R. Sessoli, and J. Villain, *Molecular Nanomagnets* (Oxford Press, New York, 2006).
 - ³ *Structure and Bonding*, Vol 122, Eds. D. M. P. Mingos, R. Winpenny (Springer, Berlin, 2006).
 - ⁴ D. Gatteschi, R. Sessoli, A. Müller, and P. Kögerler, in *Polyoxometalates: From topology via self-assembly to applications*, Eds.: M. T. Pope, A. Müller (Kluwer, Dordrecht, 2001).
 - ⁵ J. Mroziński, *Coord. Chem. Rev.* **249**, 2534 (2005).
 - ⁶ A. Müller, S. Sarkar, S.Q.N. Shah, H. Bögge, M. Schmidtman, S. Sarkar, P. Kögerler, B. Hauptfleisch, A. Trautwein, and V. Schünemann, *Angew. Chem., Int. Ed. Engl.* **38**, 3238 (1999). The complete chemical formula for $\{\text{Mo}_{72}\text{Fe}_{30}\}$ is $[\text{Mo}_{72}\text{Fe}_{30}\text{O}_{252}(\text{CH}_3\text{COO})_{12}\{\text{Mo}_2\text{O}_7(\text{H}_2\text{O})\}_2\{\text{H}_2\text{Mo}_2\text{O}_8(\text{H}_2\text{O})\}(\text{H}_2\text{O})_{91}] \cdot 150\text{H}_2\text{O}$.
 - ⁷ A. M. Todea, A. Merca, H. Bögge, J. van Slageren, M. Dressel, L. Engelhardt, M. Luban, T. Glaser, M. Henry, and A. Müller, *Angew. Chem. Int. Ed.* **46**, 6106 (2007). The complete chemical formula for $\{\text{Mo}_{72}\text{Cr}_{30}\}$ is $[\{\text{Na}(\text{H}_2\text{O})_{12}\}_C\{\text{Mo}_{72}\text{Cr}_{30}\text{O}_{252}(\text{CH}_3\text{COO})_{19}(\text{H}_2\text{O})_{94}\}] \cdot 120\text{H}_2\text{O}$.
 - ⁸ M. Axenovich and M. Luban, *Phys. Rev. B* **63**, 100407(R) (2001).
 - ⁹ A. Müller, M. Luban, C. Schröder, R. Modler, P. Kögerler, M. Axenovich, J. Schnack, P. C. Canfield, S. Bud'ko, and N. Harrison, *ChemPhysChem* **2**, 517 (2001).
 - ¹⁰ J. Schnack, M. Luban, and R. Modler, *Europhys. Lett.* **56**, 863 (2001).
 - ¹¹ The Hamiltonian operator of the Heisenberg single- J model is given by $J \sum_{\langle i,j \rangle} \vec{S}_i \cdot \vec{S}_j + g\mu_B \vec{H} \cdot \sum_i \vec{S}_i$. Here the spin operator \vec{S}_i is associated with the magnetic ions (spin s) at site i and is given in units of \hbar , the symbol $\langle i,j \rangle$ directs that the sum only includes terms associated with distinct pairs of nearest-neighbor spins, μ_B is the Bohr magneton, \vec{H} is the external magnetic field, and the theoretical result for the saturation field is⁸ $H_s = 6Js/(g\mu_B)$. The numerical values of the nearest-neighbor exchange constant J (in units of Boltzmann's constant k_B), the spectroscopic splitting factor g , and H_s are (1.57 K, 1.974, 17.7 T)⁹ and (8.7 K, 1.96, 60.0 T)⁷ for $\{\text{Mo}_{72}\text{Fe}_{30}\}$ and $\{\text{Mo}_{72}\text{Cr}_{30}\}$, respectively. The corresponding values of the exchange constants for the classical Heisenberg model are given by $J_0 = Js(s+1)$, namely 13.74 K and 32.63 K for the two molecules. The method for generating the classical Heisenberg model corresponding to a given quantum Heisenberg model is given, for example, in O. Ciftja, M. Luban, M. Auslender, and J. H. Luscombe, *Phys. Rev. B* **60**, 10122 (1999).
 - ¹² For classical spins systems that have frustrated ground states, the quantum analogs suffer from the so-called “negative sign problem” (see Ref. 13) and the quantum Monte Carlo method can provide reliable results only above a certain temperature whose value depends upon the details of the spin Hamiltonian (see Ref. 14).
 - ¹³ M. Troyer and U.-J. Wiese, *Phys. Rev. Lett.* **94**, 170201 (2005).
 - ¹⁴ L. Engelhardt, M. Luban, C. Schröder, *Phys. Rev. B* **74**, 054413 (2006).
 - ¹⁵ We have found that our probability distribution is basically the same as that employed recently in demonstrating the occurrence of a spin glass transition in a system of spins on a pyrochlore lattice with weak disorder in the strength of exchange interactions. See T. E. Saunders and J. T. Chalker, *Phys. Rev. Lett.* **98**, 157201 (2007).
 - ¹⁶ By a classical isosceles spin triangle we mean a system of three classical spins (unit vectors \vec{e}_i) described by a Hamiltonian $J(\vec{e}_1 \cdot \vec{e}_2 + \vec{e}_2 \cdot \vec{e}_3) + J'\vec{e}_3 \cdot \vec{e}_1 + (\vec{e}_1 + \vec{e}_2 + \vec{e}_3) \cdot \vec{H}$ (all quantities are dimensionless). If $J' = J$ we refer to the system as a classical equilateral spin triangle.
 - ¹⁷ C. Schröder, H. Nojiri, J. Schnack, P. Hage, M. Luban, P. Kögerler, *Phys. Rev. Lett.* **94**, 017205 (2005)
 - ¹⁸ R. Prozorov, R. W. Giannetta, A. Carrington, and F. M. Araujo-Moreira, *Phys. Rev. B* **62**, 115 (2000).
 - ¹⁹ R. Prozorov, R. W. Giannetta, A. Carrington, P. Fournier, R. L. Greene, P. Guptasarma, D. G. Hinks, and A. R. Banks, *Appl. Phys. Lett.* **77**, 4202 (2000).
 - ²⁰ M. E. Zhitomirsky, O. A. Petrenko, L. A. Prozorova, *Phys. Rev. B* **52**, 3511 (1995).
 - ²¹ V. O. Garlea, S. E. Nagler, J. L. Zarestky, C. Stassis, D. Vaknin, P. Kögerler, D. F. McMorrow, C. Niedermayer, D. A. Tennant, B. Lake, Y. Qiu, M. Exler, J. Schnack, and M. Luban, *Phys. Rev. B* **73**, 024414 (2006).
 - ²² Open-shell DFT calculations have been performed using the TURBOMOLE 5.9.1 package, see O. Treutler and R. Ahlrichs, *J. Chem. Phys.* **102**, 346 (1995). Following established routines for the broken-symmetry ansatz, TZVP-type basis sets for all elements and hybrid B3-LYP exchange-correlation functionals were used. Vanadyl (VO^{2+}) groups were chosen as they, similar to Fe^{III} and Cr^{III} in octahedral coordination environments, can be regarded as bona fide spin-only groups with virtually no zero-field splitting anisotropy effects.
 - ²³ M. Hasegawa and H. Shiba, *J. Phys. Soc. Jpn.* **73**, 2543 (2004).
 - ²⁴ R. Feyerherm, A. Loose, J. L. Manson, *J. Phys.: Condens. Matter* **15**, 663 (2003)
 - ²⁵ O. Tchernyshyov, R. Moessner, S.L. Sondhi, *Phys. Rev. B* **66**, 064403 (2002).
 - ²⁶ K. Penc, N. Shannon, H. Shiba, *Phys. Rev. Lett.* **93**, 197203 (2004).
 - ²⁷ A. Keren, J. S. Gardner, *Phys. Rev. Lett.* **87**, 177201 (2001).
 - ²⁸ S.-H. Lee, C. Broholm, W. Ratcliff, G. Gasparovic, Q. Huang, T. H. Kim, S.-W. Cheong, *Nature* **418**, 856 (2002).